

# Synthesis of nanocrystalline TiB<sub>2</sub> powder from TiO<sub>2</sub>, B<sub>2</sub>O<sub>3</sub> and Mg reactants through microwave-assisted self-propagating high-temperature synthesis method

A GHANBARI<sup>1</sup>, M SAKAKI<sup>1,\*</sup>, A FAEGHINIA<sup>2</sup>, M SH BAFGHI<sup>3,5</sup> and K YANAGISAWA<sup>4</sup>

<sup>1</sup>Department of Materials Engineering, Faculty of Engineering, Malayer University, Malayer 65719-95863, Iran

<sup>2</sup>Ceramic Division, Materials and Energy Research Center (MERC), Tehran 14155-4777, Iran

<sup>3</sup>School of Metallurgy and Materials Engineering, Iran University of Science and Technology (IUST), Narmak, Tehran 16846-13114, Iran

<sup>4</sup>Research Laboratory of Hydrothermal Chemistry, Faculty of Science, Kochi University, Kochi 780-8520, Japan

<sup>5</sup>Present address: Research Laboratory of Hydrothermal Chemistry, Faculty of Science, Kochi University, Kochi 780-8520, Japan

MS received 13 December 2015; accepted 2 February 2016

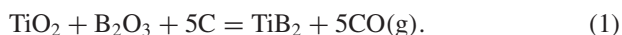
**Abstract.** In this research work, microwave-assisted self-propagating high-temperature synthesis (SHS) process was employed for the fabrication of titanium diboride (TiB<sub>2</sub>) compound from TiO<sub>2</sub>–B<sub>2</sub>O<sub>3</sub>–Mg mixtures. Thermodynamic evaluations of this system and its relevant subsystems revealed that TiB<sub>2</sub>–MgO composite powder can be easily produced by a SHS reaction. However, experimental results of a TiO<sub>2</sub> : B<sub>2</sub>O<sub>3</sub> : 5Mg mixture heated in a domestic oven showed the formation of some intermediate compounds such as Mg<sub>3</sub>B<sub>2</sub>O<sub>6</sub>, presumably due to some degree of Mg loss. The optimum amount of Mg in TiO<sub>2</sub> : B<sub>2</sub>O<sub>3</sub> : xMg mixtures, yielding the highest amount of TiB<sub>2</sub> phase, was found to be around 7 mol, i.e., 40 mol% more than the stoichiometric amount. Experimental results revealed that a pure TiB<sub>2</sub> compound could be obtained by leaching the unwanted by-products in an HCl acid solution. Scanning electron microscopic observations and Scherrer calculations showed that the produced TiB<sub>2</sub> contains sub-micron (150–200 nm) particles, where each particle consists of a number of nanosized (32 nm) crystallites.

**Keywords.** Titanium diboride; thermodynamic calculations; microwave processing; combustion synthesis.

## 1. Introduction

Titanium diboride (TiB<sub>2</sub>), the most stable intermetallic compound of titanium and boron, has excellent properties such as high melting point and hardness, good thermal conductivity and stability together with high chemical and abrasive resistance. It can be used as cutting tools, abrasives, turbine blades as well as a cathode in aluminium smelting. As a reinforcement agent, TiB<sub>2</sub> improves the mechanical properties of sintered bodies [1–4].

TiB<sub>2</sub> can be commercially synthesized by carbothermic reduction of a TiO<sub>2</sub>–B<sub>2</sub>O<sub>3</sub> mixture (equation (1)). This method requires a long time heating at high temperatures which makes the process very costly, therefore [5,6]



In recent times, some inexpensive methods/reagents have been proposed for the synthesis of TiB<sub>2</sub> compound, including chemical vapour deposition [7], sol–gel processing [8], solvothermal synthesis [9], mechanical alloying [10], thermal plasma process [11] and self-propagating high-temperature synthesis (SHS) method.

The last method (SHS) named also as combustion synthesis (CS), utilizes the exothermicity of chemical reactions to promote the synthesis process [12–15]. To predict the possibility of use of SHS technique for the synthesis of a compound, thermodynamic calculations are of a noticeable help [16,17]. According to Merzhanov's criterion, the type of reaction is SHS, if its adiabatic temperature ( $T_{\text{ad}}$ : highest temperature of the system under adiabatic condition) is higher than 1800 K [16]. In general, SHS reactions are triggered by using: (i) a furnace or (ii) an electrical element touching the surface of a green sample. Some advantages of SHS route can be summarized as: high production rate, simplicity, low energy consumption and good purity of the products [12,13]. SHS method has been recognized as a promising synthesis method for the fabrication of various advanced ceramics, e.g., carbides, nitrides and borides.

SHS synthesis of TiB<sub>2</sub> composite materials containing either MgO or Al<sub>2</sub>O<sub>3</sub> from TiO<sub>2</sub>–(B<sub>2</sub>O<sub>3</sub>/H<sub>3</sub>BO<sub>3</sub>)–(Mg/Al) reagents has been studied by various research groups [18–29]. It has been found that a SHS reaction gets promoted if Mg is used as the reducing agent [23]; while in the case of Al, addition of a mechanical activation step is necessary for the successful reaction ignition [30]. Moreover, it has been shown that some by-product phases, such as Mg<sub>3</sub>B<sub>2</sub>O<sub>6</sub>, Mg<sub>2</sub>TiO<sub>4</sub>, AlB<sub>2</sub> and TiAl<sub>3</sub> could be formed [23,25,26]. These

\*Author for correspondence (masoudsakaki79@gmail.com, masoud\_sakaki@iust.ac.ir)

unwanted phases can be reduced or eliminated by precise control of the initial composition of reactants mixture as well as proper adjustment of synthesis conditions [23,25]. Moreover, addition of diluents such as NaCl results in a lower adiabatic temperature with the consequence of grain refinement of the final product [27]. It has been reported that use of Mg as the reducing agent is preferred for the fabrication of pure  $TiB_2$  phase due to the ease of elimination of MgO through acid leaching of  $TiB_2$ -MgO powder [29].

In recent times, microwave energy has been used for triggering the SHS systems [31–34]. Since in microwave heating, heat is generated within the materials, it is totally different from the conventional heating methods. Internal heat generation during microwave heating brings about a uniform heat distribution in the samples, resulting in a more homogeneous product. Other advantages of microwave energy as the heating source are ability of selective heating, shortening the time/cost of the process together with less environmental pollution [35–37]. The efficiency of microwave heating is controlled by heat conductivity and dielectric properties of the target, microwave frequency and power, as well as operating temperature [38,39].

Microwave-assisted SHS synthesis of  $TiB_2$ - $Al_2O_3$  composite powder has been reported by Farhadinia [40] and Mousavian [41]. They have shown that for a successful synthesis, mechanical activation of reagents is required. Since leaching of  $Al_2O_3$  phase from the fabricated  $TiB_2$ - $Al_2O_3$  composite is not a simple process, production of a pure  $TiB_2$  phase cannot be easily achieved. It would be reasonable therefore, to search for other convenient reducing agents.

In this research work, production of nanocrystalline  $TiB_2$  phase from  $TiO_2$ - $B_2O_3$ -Mg reagents through microwave-assisted SHS synthesis route has been studied. Thermodynamic calculations were used for the prediction of the behaviour of possible reactions. Several synthesis experiments were performed in a domestic microwave oven to find out the optimum initial composition. In addition, to produce a pure  $TiB_2$  phase, by-product compounds were leached away by using a dilute HCl solution. Microstructure of the optimum product was examined by a scanning electron microscope (SEM) and its crystallite size was evaluated by applying the Scherrer equation [42].

## 2. Experimental

The aim of this study is the production of pure  $TiB_2$  phase through microwave-assisted SHS reaction. Thermodynamic calculations were performed to predict the possibility as well as the mode of probable reactions. For this purpose,  $\Delta G^0$ ,  $\Delta H^0$  and  $T_{ad}$  values have been computed by the use of available thermodynamic data [43].

Experimental investigations were performed using analytical grade  $TiO_2$ ,  $B_2O_3$  and Mg powders. Reagents were mixed by hand and pressed into green cylindrical samples (10 mm diameter and 4 mm height) by an axial hydraulic pressing device.

Microwave heating was performed by use of a domestic microwave oven (Samsung: GE2370G, 850 W output power). Since the capability of the green samples for absorption of microwave energy was unacceptably low, a block of microwave energy absorbing silicon carbide (SiC) was located under the samples to promote the synthesis process. Figure 1 represents the schematic illustration of the experimental set-up. Our investigations and experiences showed that  $Al_2O_3$  and  $SiO_2$  are transparent to microwave radiation and therefore, would not affect the heating efficiency. They were merely used to prevent air infiltration to the reaction vicinity.

Samples were heated-up to initiate SHS reaction. Observation of specific physical phenomena (e.g., flaming and flushing of samples) were the signs of reaction occurrence and progress. After SHS reaction, microwave device was turned off and the set-up was left to be cooled down slowly. Produced powder was grounded in an alumina mortar and its composition was identified by an X-ray diffraction instrument (XRD: Unisantix-XMD 300,  $CuK\alpha$  radiation). Acid leaching step was done by a dilute HCl solution under a moderate stirring condition. The temperature and stirring time were fixed at 50°C and 2 h, respectively.

Microstructure and chemical composition of the product were evaluated by a SEM machine (TESCAN-VEGA II) equipped with an energy-dispersive X-ray spectrometer (EDX). For this purpose, the powder was dispersed in ethanol by ultrasonic vibration. Then, one droplet of the suspension was placed on a piece of glass, which will be coated with Au after the ethanol evaporation.

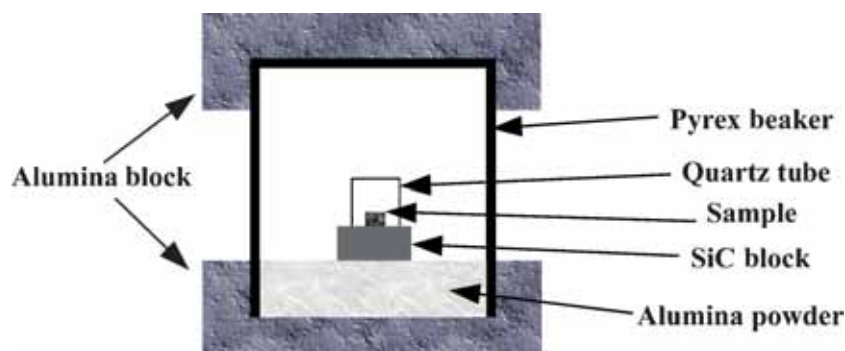


Figure 1. Schematic of the experimental set-up.

Crystallite size of the product was calculated by use of the Scherrer equation

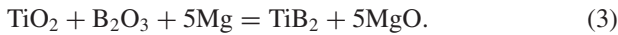
$$d = 0.9\lambda / [(\beta \cdot \cos(\theta))], \quad (2)$$

where  $d$  is the crystallite size,  $\lambda$  the wavelength of X-ray radiation,  $\beta$  the peak width at half-maximum height and  $\theta$  the diffraction angle.

### 3. Results and discussion

#### 3.1 Thermodynamic calculations

The overall reaction in  $TiO_2$ - $B_2O_3$ -Mg system could be written as follows:



In fact, equation (3) is the sum of magnesiothermic reduction reactions of  $TiO_2$  and  $B_2O_3$  (equations (4) and (5)) together with the reaction between reduced Ti and B (equation (6)).



To gain an insight into equation (3), values of  $\Delta G^0$ ,  $\Delta H^0$  and  $T_{ad}$  of its sub-reactions (i.e., equations (4)–(6)) were calculated. The results are presented in the following sections.

3.1a  $TiO_2$ -Mg system: Transformation temperature of starting materials and products of equations (4)–(6) should be taken into account during thermodynamic calculations. Table 1 shows these phase change temperatures. Figure 2a

**Table 1.** Possible phase transformations of raw materials and products of equations (4)–(6).

Transformation	Temperature (K)
$B_2O_3 (s) \leftrightarrow B_2O_3 (l)$	723
$Mg (s) \leftrightarrow Mg (l)$	923
$Ti (s_1) \leftrightarrow Ti (s_2)$	1166
$Mg (l) \leftrightarrow Mg (g)$	1367
$Ti (s_2) \leftrightarrow Ti (l)$	1939
$TiO_2 (s) \leftrightarrow TiO_2 (l)$	2130
$B_2O_3 (l) \leftrightarrow B_2O_3 (g)$	2330
$B (s) \leftrightarrow B (l)$	2350
$MgO (s) \leftrightarrow MgO (l)$	3098
$TiB_2 (s_1) \leftrightarrow TiB_2 (s_2)$	3193
$Ti (l) \leftrightarrow Ti (g)$	3634
$MgO (l) \leftrightarrow MgO (g)$	3771
$TiO_2 (l) \leftrightarrow TiO_2 (g)$	3801
$B (l) \leftrightarrow B (g)$	4143

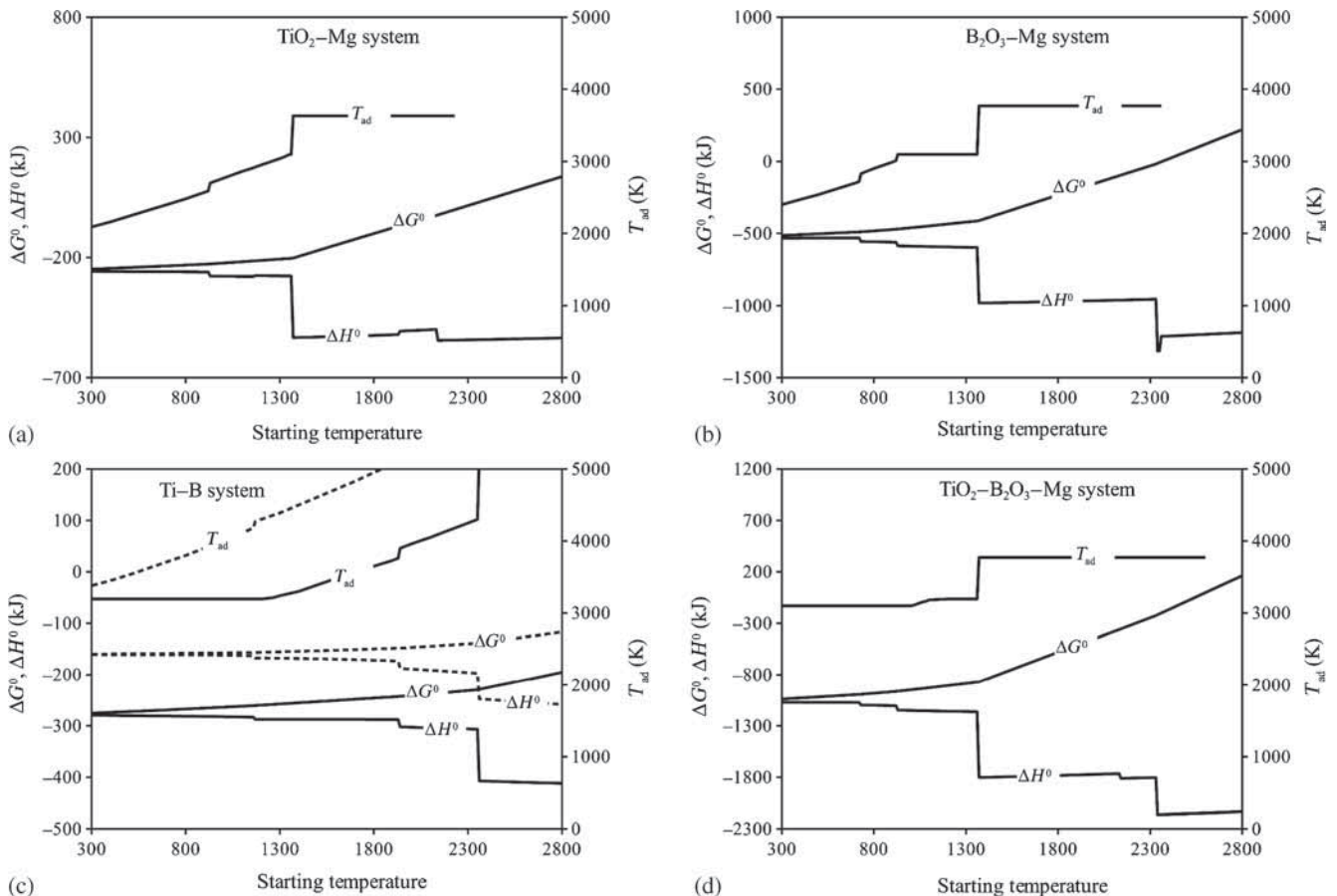


**Figure 2.**  $\Delta G^0$ ,  $\Delta H^0$  and  $T_{ad}$  values of equations (3)–(7) vs. the starting temperature.

represents the values of  $\Delta G^0$ ,  $\Delta H^0$  and  $T_{ad}$  of equation (4) as a function of the starting temperature. Observed breaks at 923, 1166, 1367, 1939, 2130, 3098 and 3634 K are related to the phase transitions of Mg, Ti,  $TiO_2$  and MgO, according to table 1.  $\Delta G^0$  of equation (4) at 300 K is  $-248.9 \text{ kJ mol}^{-1}$ , which is an indication of its high tendency for propagation. Although, the increase of  $\Delta G^0$  by increasing the starting temperature indicates the reverse effect of temperature, negative values of  $\Delta G^0$  in 300–2230 K range show that the reduction of  $TiO_2$  by Mg is still possible in this range. According to figure 2a, equation (4) becomes thermodynamically impossible above 2230 K. As figure 2a shows, equation (4) is very exothermic ( $\Delta H^0 = -258.2 \text{ kJ mol}^{-1}$ ) at 300 K. Hence, it is expected that the temperature of whole mixture would be increased as a consequence of reaction propagation. Calculated results (figure 2a) confirm this expectation showing that  $T_{ad}$  of equation (4) starting from 300 K, is as high as 2090 K. Therefore, the type of equation (4) is SHS, according to Merzhanov's criterion [16]. Figure 2a also shows that the exothermicity of equation (4) goes higher by increasing the starting temperature. This in turn brings about a higher adiabatic temperature in the system. According to figure 2a, when the starting temperature of the system is higher than 1370 K,  $T_{ad}$  reaches to 3634 K and then remains constant, expectedly as the consequence of liquid to gas phase transformation of reduced titanium (see table 1).  $T_{ad}$  has not been calculated for starting temperatures beyond 2230 K, because equation (4) becomes thermodynamically impossible, thereafter.

**3.1b  $B_2O_3$ -Mg system:** Curves of  $\Delta G^0$ ,  $\Delta H^0$  and  $T_{ad}$  of equation (5) vs. starting temperature are shown in figure 2b. Again, breaks in figure 2b are related to the relevant phase transformations shown in table 1.  $\Delta G^0$  value at 300 K is  $-514.7 \text{ kJ}$  indicating the inherent tendency of the reaction to go forward. By increasing the initial temperature,  $\Delta G^0$  value increases which is unfavourable for the reaction progress.  $\Delta G^0$  value becomes positive at temperatures higher than 2360 K indicating that the reaction is impossible at such high temperature as per the thermodynamic viewpoint.

On the other hand, figure 2b reveals that at 300 K, equation (5) is very exothermic ( $\Delta H^0 = -532.6 \text{ kJ}$ ) and its adiabatic temperature is around 2400 K. Hence, according to Merzhanov's criterion, the reaction would be of a SHS type. Similar to the  $TiO_2$ -Mg system, by increasing the initial temperature, the exothermicity degree and adiabatic temperature of equation (5) were increased. Figure 2b shows that the adiabatic temperature reaches to 3771 K, when the initial temperature was 1370 K.

**3.1c Ti-B system:** Regarding the above thermodynamic calculations,  $TiO_2$  and  $B_2O_3$  are expected to be easily reduced by Mg during microwave heating of  $TiO_2$ - $B_2O_3$ -Mg mixture. The reaction between reduced Ti and B (i.e., equations (6) and (7)) is examined, hereinafter



Figure 2c shows the calculated values of  $\Delta G^0$ ,  $\Delta H^0$  and  $T_{ad}$  of equations (6) and (7) as a function of starting temperature. In this figure, continuous and dashed lines represent data belonging to equations (6) and (7), respectively. Considering this figure in conjunction with previous explanations, both reactions are thermodynamically possible and are exothermic. Values of  $T_{ad}$  of equations (6) and (7) are higher than 1800 K; therefore, both reactions are expected to proceed with a combustion mode. It is notable that for the whole range of starting temperature,  $\Delta G^0$  value of equation (6) is lower than that of equation (7). Moreover, equation (6) is more exothermic. Hence, it can be concluded that the production of  $TiB_2$  (through equation (6)) is thermodynamically preferred.

**Conclusion of thermodynamic evaluations:** A comparison of figure 2a and b reveals that in  $TiO_2$ - $B_2O_3$ -Mg mixture, the chemical reaction is expected to be initiated by equation (5), which has a more negative  $\Delta G^0$  value compared to equation (4). Afterwards, released heat of equation (5) will activate equations (4) and (6). In other words,  $TiB_2$ -MgO composite will be formed through equation (3). The  $\Delta G^0$ ,  $\Delta H^0$  and  $T_{ad}$  values of equation (3) are plotted in figure 2d, as a function of starting temperature. With regard to  $\Delta G^0$  curve, the occurrence possibility of equation (3) in  $TiO_2$ - $B_2O_3$ -Mg mixture is very high. Equation (3) is extremely exothermic, so that its type is SHS, according to Merzhanov's criterion. Hence, it could be concluded that from the thermodynamic standpoint,  $TiB_2$ -MgO composite can be easily produced through the microwave-assisted SHS method.

### 3.2 Experimental findings

A summary of mixture compositions, heating times and experimental observations of all investigated samples is presented in table 2. Figure 3 shows an example of the shape of a typical sample, before and after the SHS reaction. The figure shows that after the combustion reaction, the volume of the initial compact has considerably increased and the product has gained a layered structure. These phenomena that have been observed in other SHS reaction studies, are supposed to be a physical consequence of the evolution of gaseous products from the compact at high system temperatures [44].

Figure 4a exhibits the XRD pattern of a sample obtained by heating  $TiO_2 : B_2O_3 : 5Mg$  mixture. No evidence of the starting materials is visible in this figure and the main detectable phases are MgO and  $TiB_2$ . The existence of MgO

**Table 2.** Composition, ignition time ( $t_{ig}$ ) and mode of reaction for various investigated  $TiO_2$ - $B_2O_3$ -Mg systems.

Sample code	Composition	$t_{ig}$ (s)	Reaction type
A	$TiO_2 : B_2O_3 : 5Mg$	38	SHS
B	$TiO_2 : B_2O_3 : 6Mg$	57	SHS
C	$TiO_2 : B_2O_3 : 7Mg$	92	SHS
D	$TiO_2 : B_2O_3 : 8Mg$	97	SHS

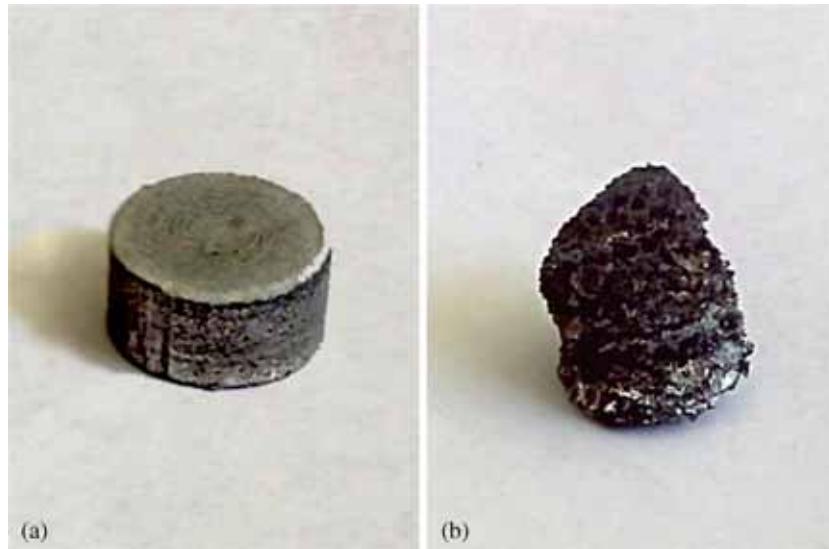


**Figure 3.** Shape of a typical sample (a) before and (b) after the SHS reaction.

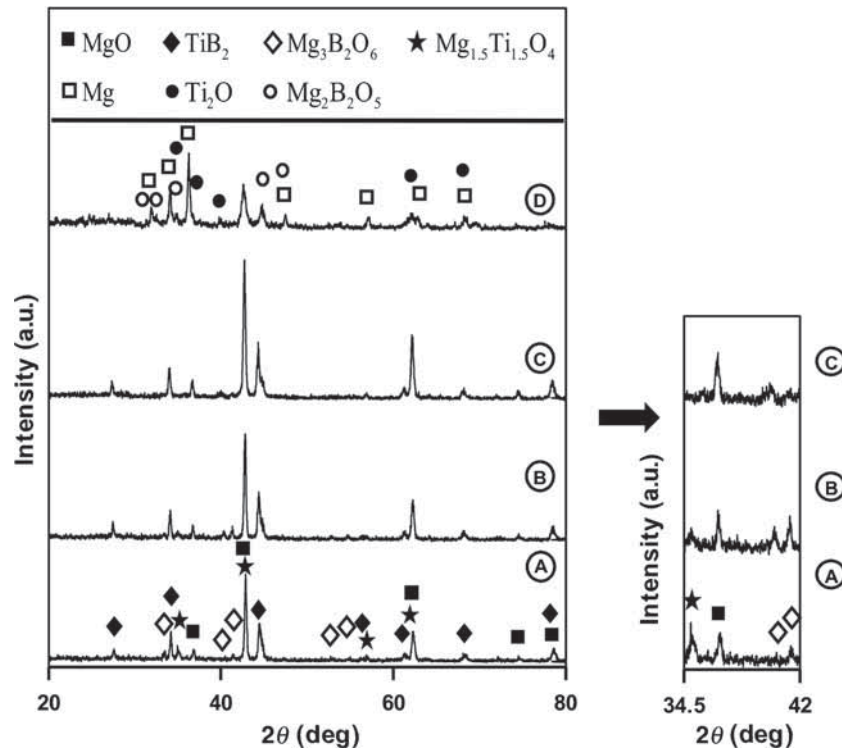


**Figure 4.** XRD patterns of heated  $TiO_2 : B_2O_3 : xMg$  mixtures. A:  $x = 5$ , B:  $x = 6$ , C:  $x = 7$  and D:  $x = 8$ . The 34.5–42 degree portion of the patterns A–C are separately shown with a higher magnification. The employed JCPDF cards for phase identification are:  $MgO$ : 00-004-0829,  $TiB_2$ : 00-008-0121,  $Mg_3B_2O_6$ : 00-038-1475,  $Mg_{1.5}Ti_{1.5}O_4$ : 00-044-0086,  $Mg$ : 00-035-0821,  $Ti_2O$ : 00-011-0218 and  $Mg_2B_2O_5$ : 00-016-0168.

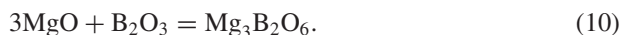
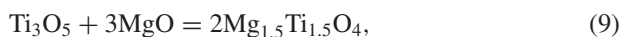
phase confirms the occurrence of magnesiothermic reduction reactions (equations (4) and (5)). Reaction type in this system has been SHS (see table 2), which is in agreement with the thermodynamic predictions. According to equation (3), it is expected that heating of  $TiO_2 : B_2O_3 : 5Mg$  mixture will yield a  $TiB_2$ – $MgO$  composite powder. However, other

by-products (such as  $Mg_3B_2O_6$ ) are visible in figure 4a, whose existence could be attributed to Mg deficiency in the system due to the following phenomena:

- (i) Partial oxidation of Mg as a result of some oxygen leakage into the reaction chamber.

- (ii) Partial escape of vapourized magnesium (boiling point = 1367 K) at high system temperatures.

Mg deficiency causes incomplete reduction of initial oxide phases. Hence, some  $\text{TiO}_2$  and  $\text{B}_2\text{O}_3$  reagents remain in the system. By-products observable in figure 4a, are supposed to be formed as a result of the reaction of MgO (produced in reduction reactions) with the remained  $\text{TiO}_2$  and  $\text{B}_2\text{O}_3$  oxides



According to the above justification,  $\text{Mg}_3\text{B}_2\text{O}_6$  and  $\text{Mg}_{1.5}\text{Ti}_{1.5}\text{O}_4$  formations could be prevented by use of higher Mg amounts in the  $\text{TiO}_2$ - $\text{B}_2\text{O}_3$ -Mg mixture.

Table 2 shows that the reactions type has not been affected by the amounts of Mg in  $\text{TiO}_2 : \text{B}_2\text{O}_3 : x\text{Mg}$  mixtures, so that all reactions have SHS behaviour. Nevertheless, due to the microwave radiation reflection by metals [37], it is expected that by increasing the metal content in the mixture, the energy absorption efficiency and consequently the system temperature will be decreased; causing a delay in SHS reaction initiation. Confirmation proof of this postulation is seen in table 2.

Figure 4b–d shows the XRD patterns of samples, synthesized by various amounts of Mg in  $\text{TiO}_2 : \text{B}_2\text{O}_3 : x\text{Mg}$  mixtures. By increasing the initial Mg content from 1 to 1.4 times of its stoichiometric amount (i.e., from 5 to 7 moles) the peak heights (intensities) of by-products have decreased (compare patterns A, B and C). Considering the proposed reaction mechanism, this phenomenon is probably due to further reduction of  $\text{B}_2\text{O}_3$  and  $\text{TiO}_2$ , which diminishes equations (8)–(10). The promising effect of increasing Mg contents of  $\text{TiO}_2 : \text{B}_2\text{O}_3 : x\text{Mg}$  mixtures on the formation of  $\text{TiB}_2$  compound could also be seen in figure 5, where  $I_{\text{preferred phase}}/I_{\text{unwanted phases}}$  has been used as a scale for the evaluation of overall reaction (equation (3)) completeness.

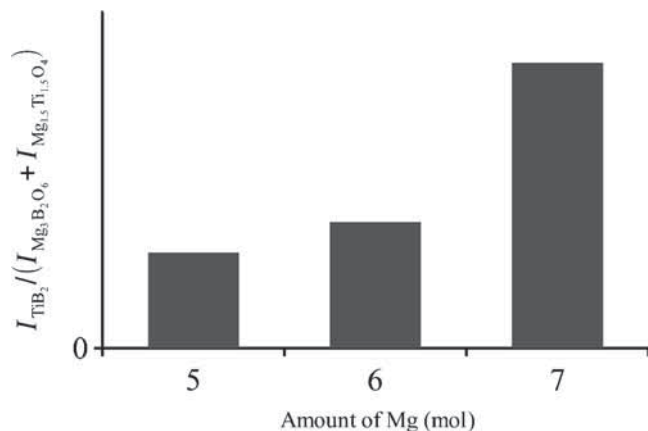


**Figure 5.** Effect of initial Mg amounts in  $\text{TiO}_2 : \text{B}_2\text{O}_3 : x\text{Mg}$  mixtures on the  $I_{\text{preferred phase}}/I_{\text{unwanted phase}}$  ratio.

The presence of unwanted by-products in the pattern 4-C reveals that the use of higher Mg amounts is necessary. Nevertheless, by using 8 moles of magnesium (i.e., 1.6 times of the stoichiometric amount) peaks of by-products are still observable in the XRD pattern (figure 4d), together with peaks of unreacted magnesium. A possible reason may be the reflective characteristic of Mg towards microwave energy that prevents the whole system from effective energy absorption; so that the reaction cannot take place completely and some Mg remains unreacted. Therefore, it may be concluded that the optimum amount of Mg in  $\text{TiO}_2 : \text{B}_2\text{O}_3 : x\text{Mg}$  mixtures, which yields the highest amount of  $\text{TiB}_2$  and the lowest amounts of unwanted by-products, is around about 1.4 times of the stoichiometric amount.

To produce a pure  $\text{TiB}_2$  compound, the product obtained from the heating of  $\text{TiO}_2 : \text{B}_2\text{O}_3 : 7\text{Mg}$  mixture was leached

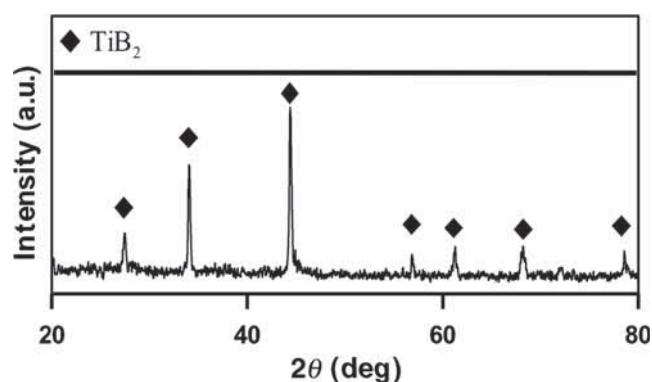


**Figure 6.** XRD pattern of pure  $\text{TiB}_2$  phase (JCPDF card: 00-008-0121) obtained by acid leaching of the  $\text{TiO}_2 : \text{B}_2\text{O}_3 : 7\text{Mg}$  system reaction product.

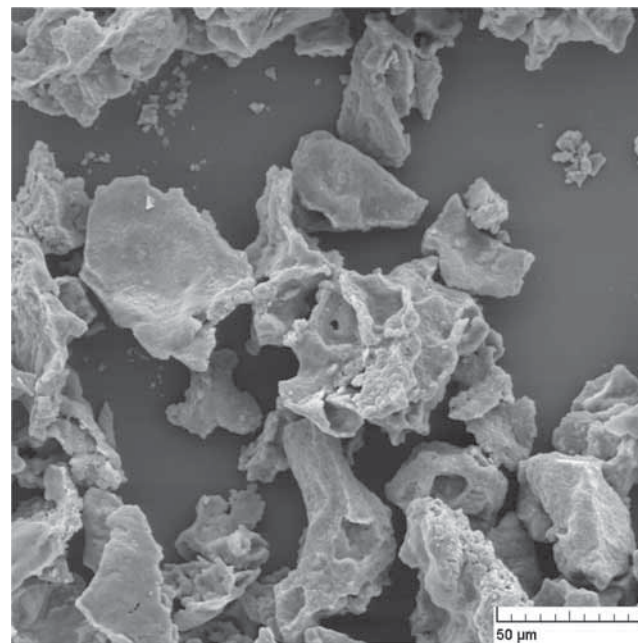


**Figure 7.** SEM image (1000 $\times$ ) of  $\text{TiO}_2 : \text{B}_2\text{O}_3 : 7\text{Mg}$  system reaction product.

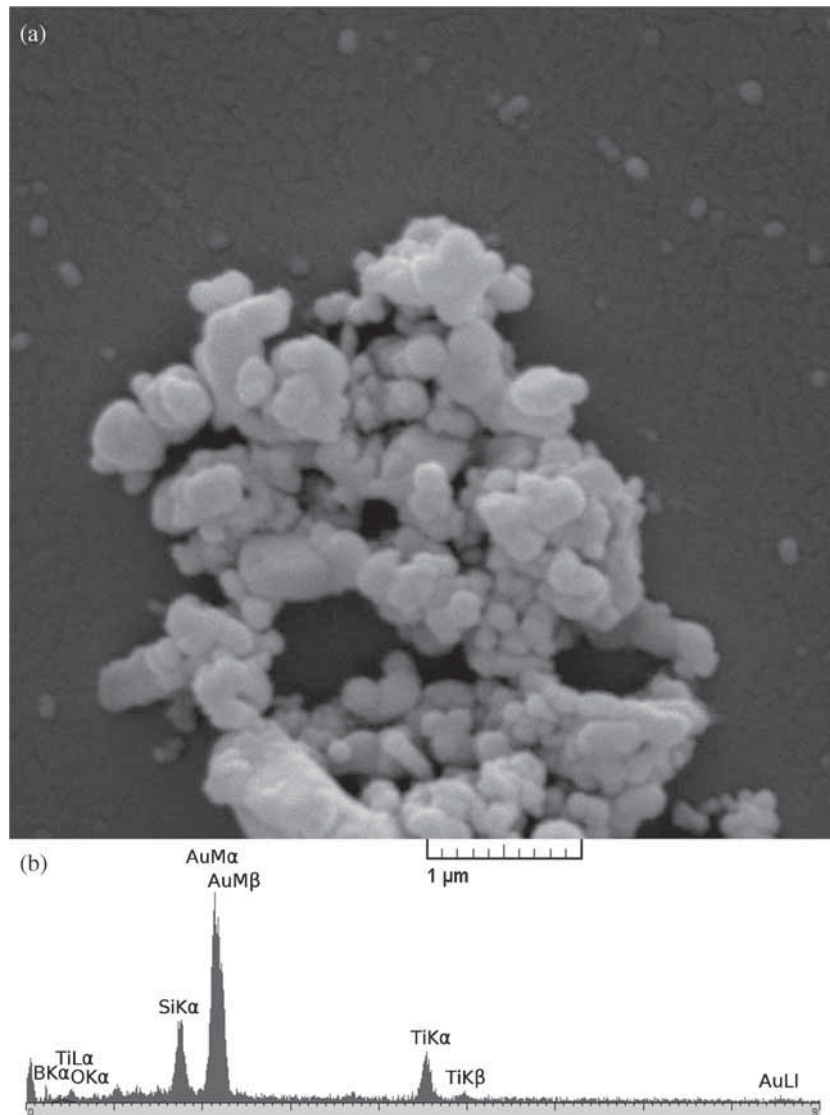


**Figure 8.** (a) SEM image (40,000 $\times$ ) and (b) EDX data of the acid leached product of  $TiO_2 : B_2O_3 : 7Mg$  system.

in a dilute HCl solution. Figure 6 displays the XRD pattern of a heated  $TiO_2 : B_2O_3 : 7Mg$  sample after acid leaching. It could be seen that all by-product compounds have been successfully eliminated and the remaining powder is solely a  $TiB_2$  phase.

### 3.3 Morphology and microstructure

Figure 7 shows the SEM image of a  $TiO_2 : B_2O_3 : 7Mg$  mixture, after the SHS reaction. As can be seen, the product consists of large agglomerates. Probably, the high temperature of SHS reaction has caused some partial sintering and agglomeration [31].

The SEM image of heated and leached  $TiO_2 : B_2O_3 : 7Mg$  mixture is presented in figure 8a, where the mean particle size is estimated as in the range of 150–200 nm. Formation of these fine (sub-micron) particles from the very large initial agglomerates (figure 7) can be attributed to the

**Table 3.** Calculated crystallite size of produced  $TiB_2$  phase.

$2\theta$ (deg)	Crystallite size (nm)
27.47	30.1
34.06	33.5
44.38	30.3
61.23	32.6

Note: Mean crystallite size (nm): 31.6.

boundary breakage during the acid leaching process [45,46]. Figure 8b shows the result of EDX analysis of the mentioned sample. Si, O and Au peaks in EDX analysis data are originated from the base glass and Au coating used for sample preparation. The absence of Mg peak in the EDX result is in agreement with figure 6, demonstrating the effectiveness of acid leaching practice for the complete elimination of unwanted phases from the product.

Table 3 shows the diffraction angles and crystallites sizes of the produced TiB<sub>2</sub> phase calculated by using four main peaks of figure 6. The mean crystallite size of TiB<sub>2</sub> phase is found to be around 32 nm.

#### 4. Conclusion

The aim of this research work has been the investigation of the possibility of fabrication of TiB<sub>2</sub> compound from TiO<sub>2</sub>-B<sub>2</sub>O<sub>3</sub>-Mg mixture through microwave-assisted SHS in a low power (domestic) oven. Summary of thermodynamic evaluations and experimental findings are as follows:

- (1) Over a wide range of starting temperature, magnesiothermic reduction of TiO<sub>2</sub> and B<sub>2</sub>O<sub>3</sub> via SHS reaction is thermodynamically possible. Titanium diboride is formed thereafter, through the reaction between the reduced Ti and B.
- (2) Experimental investigation of TiO<sub>2</sub> : B<sub>2</sub>O<sub>3</sub> : 5Mg system showed that although TiB<sub>2</sub>-MgO composite is formed in this system, the product contains some amounts of unwanted intermediate phases such as Mg<sub>3</sub>B<sub>2</sub>O<sub>6</sub>, whose formation presumably is originated from some degree of Mg deficiency in the system. It is believed that Mg deficiency is the result of magnesium loss due to either Mg vapourization at high system temperatures or its oxidation by infiltrated oxygen (air).
- (3) Experimental investigations about TiO<sub>2</sub> : B<sub>2</sub>O<sub>3</sub> : xMg mixtures showed that with the increase of initial Mg amounts up to 7 mol (40 mol% excess), the amount of TiB<sub>2</sub> phase in the product increases.
- (4) Leaching in a dilute HCl acid solution was found effective for the purification of TiO<sub>2</sub> : B<sub>2</sub>O<sub>3</sub> : 7Mg system product and obtaining a pure TiB<sub>2</sub> phase.
- (5) SEM observations showed that the products of SHS reactions are in the form of sintered, large and dense agglomerates, which consist of sub-micron TiB<sub>2</sub> particles.
- (6) Scherrer calculations showed that the mean crystallite size of the produced TiB<sub>2</sub> is about 32 nm.
- (7) Good agreement was found between theoretical predictions and experimental findings.

#### References

- [1] Wang H Y, Jiang Q C, Zhao Y Q, Zhao F, Ma B X and Wang Y 2004 *Mater. Sci. Eng. A* **372** 109
- [2] Tang W M, Zheng Z X, Wu Y C, Wang J M, Lu J and Liu J W 2006 *Trans. Nonferrous Met. Soc. China* **16** 613
- [3] Ziemnicka-Sylwester M 2013 *Materials* **6** 1903
- [4] Königshofer R, Fürsinn S, Steinkellner P, Lengauer W, Haas R, Rabitsch K and Scheerer M 2005 *Int. J. Refract. Met. Hard Mater.* **23** 350
- [5] Ivanov V V, Blokhina I A and Kirik S D 2014 *Russ. J. Appl. Chem.* **86** 1650
- [6] Kang S H and Kim D J 2007 *J. Eur. Ceram. Soc.* **27** 715
- [7] Pierson H O and Mullendore A W 1982 *Thin Solid Films* **95** 99
- [8] Bača L' and Stelzer N 2008 *J. Eur. Ceram. Soc.* **28** 907
- [9] Gu Y, Qian Y, Chen L and Zhou F 2003 *J. Alloys Compd.* **352** 325
- [10] Hwang Y and Lee J K 2002 *Mater. Lett.* **54** 1
- [11] Cheng Y, Shigeta M, Choi S and Watanabe T 2012 *Chem. Eng. J.* **183** 483
- [12] Patil K C, Aruna S T and Mimani T 2002 *Curr. Opin. Solid State Mater. Sci.* **6** 507
- [13] Varma A and Mukasyan A S 2004 *Korean J. Chem. Eng.* **21** 527
- [14] Liu G, Li J and Chen K 2013 *Int. J. Refract. Met. Hard Mater.* **39** 90
- [15] Sangshetti R M, Hiremath V A and Jali V M 2011 *Bull. Mater. Sci.* **34** 1027
- [16] Novikov N P, Borovinskaya I P and Merzhanov A G 1975 *Combustion process in chemical technology metallurgy* (ed) A G Merzhanov (Chernogolovka, Moscow) p 174
- [17] Moore J J and Feng H J 1995 *Prog. Mater. Sci.* **39** 243
- [18] Yeh C L and Li R F 2009 *Chem. Eng. J.* **147** 405
- [19] Nozari A, Ataie A and Heshmati-Manesh S 2012 *Mater. Charact.* **73** 96
- [20] Li J, Cai Z, Guo H, Xu B and Li L 2009 *J. Alloys Compd.* **479** 803
- [21] Meyers M, Olevsky E, Ma J and Jamet M 2001 *Mater. Sci. Eng. A* **311** 83
- [22] Mishra S K, Gokuul V and Paswan S 2014 *Int. J. Refract. Met. Hard Mater.* **43** 19
- [23] Weimin W, Zhengyi F, Hao W and Runzhang Y 2002 *J. Mater. Process. Technol.* **128** 162
- [24] Niyomwas S, Chaichana N, Memongkol N and Wannasin J 2008 *Songklanakarinn J. Sci. Technol.* **30** 233
- [25] Bilgi E, Çamurlu H E, Akgün B, Topkaya Y and Sevinç N 2008 *Mater. Res. Bull.* **43** 873
- [26] Wang H Y, Jiang Q C, Zhao Y G and Zhao F 2004 *J. Alloys Compd.* **379** 4
- [27] Khanra A K, Pathak L C, Mishra S K and Godkhindi M M 2004 *Mater. Lett.* **58** 733
- [28] Derin B, Demircan U and Yücel O 2007 *Metall. Mater. Eng.* **4** 47
- [29] Demircan U, Derin B and Yücel O 2007 *Mater. Res. Bull.* **42** 312
- [30] Aminikia B 2013 *Chiang Mai J. Sci.* **40** 274
- [31] Sakaki M, Karimzadeh Behnami A and Bafghi M S 2014 *Int. J. Refract. Met. Hard Mater.* **44** 142
- [32] Hoseinpour A, Bafghi M Sh, Vahdati Khaki J, Jalaly M and Sakaki M 2015 *Int. J. Refract. Met. Hard Mater.* **50** 191
- [33] Ganesh I, Johnson R, Rao G V N, Mahajan Y R, Madavendra S S and Reddy B M 2005 *Ceram. Int.* **31** 67
- [34] Mangalaraja R V, Ramam K V S, Ravi J and Camurri C P 2007 *Mater. Sci. Pol.* **25** 1075
- [35] Jones D A, Lelyveld T P, Mavrofidis S D, Kingman S W and Miles N J 2002 *Resour. Conserv. Recycl.* **34** 75
- [36] Chandrasekaran S, Ramanathan S and Basak T 2012 *AIChE J.* **58** 330

- [37] Thostenson E T and Chou T-W 1999 *Composites Part A: Appl. S.* **30** 1055
- [38] Haque K E 1999 *Int. J. Miner. Process.* **57** 1
- [39] Agrawal D K 1998 *Curr. Opin. Solid State Mater. Sci.* **3** 480
- [40] Farhadinia F and Sedghi A 2014 *Metall. Mater. Trans. A* **45** 3125
- [41] Mousavian R T, Sharafi S and Shariat M H 2011 *Int. J. Refract. Met. Hard Mater.* **29** 281
- [42] Cullity B D and Stock S R 1978 *Elements of X-ray diffraction* (Massachusetts, USA: Addison-Wesley)
- [43] [http://www.crct.polymtl.ca/reactweb\\_plus.php](http://www.crct.polymtl.ca/reactweb_plus.php)
- [44] Lee J H, Seo D H, Won C W, Borovinskaya I P and Vershinnikov V I 2001 *J. Mater. Sci.* **36** 5311
- [45] Aruna S T and Mukasyan A S 2008 *Curr. Opin. Solid State Mater. Sci.* **12** 44
- [46] Borovinskaya I P, Ignat T I, Vershinnikov V I, Khurtina G G and Sachkova N V 2003 *Inorg. Mater.* **39** 588